ELSEVIER

Physica A 311 (2002) 339–352

PHYSICA A

www.elsevier.com/locate/physa

Adsorption of dimers on heterogeneous surfaces: scaling behavior for the adsorption isotherms

J.E. González[a], A.J. Ramirez-Pastor[b,*]

[a] *Departamento de Física, Facultad de Ingeniería, Universidad Nacional de San Juan, Av. Libertador Gral. San Martín 1109-Oeste, 5400 San Juan, Argentina*

[b] *Departamento de Física, Laboratorio de Ciencias de Superficie y Medios Porosos and Centro Latinoamericano de Estudios Ilya Prigogine, Universidad Nacional de San Luis, CONICET, Chacabuco 917, 5700 San Luis, Argentina*

Received 26 November 2001; received in revised form 20 February 2002

Abstract

The localized monolayer adsorption of homonuclear dimers on heterogeneous surfaces with simple topographies is analyzed by combining theoretical modeling and Monte Carlo (MC) simulations. The heterogeneous surfaces are represented by lattices with two kinds of sites, the so-called bivariate heterogeneous surface. Shallow and deep sites with energies ε_S and ε_D, respectively, form $l \times l$ patches distributed at random or in chessboard-like ordered domains on two-dimensional square, honeycomb and triangular lattices. The adsorption process is monitored by following the adsorption isotherms. The scope of the present work is to determine, via MC simulation and a theoretical model, the general properties of the adsorption of non-interacting dimers on bivariate surfaces with a characteristic correlation length, l. These findings are discussed for the determination of the energetic topography of the surface, from adsorption measurements.

PACS: 68.43.−h; 82.65.+r; 34.50.Dy; 02.70.Uu

Keywords: Adsorption; Multisite occupancy; Heterogeneous surfaces; Monte Carlo simulations

1. Introduction

The problem of calculating the multiplicity of arrangements of indistinguishable dimers distributed on a lattice [1–3] has its origin in the statistical treatment of

* Corresponding author. Tel.: +54-2652-436151; fax: +54-2652-430224.
E-mail address: antorami@unsl.edu.ar (A.J. Ramirez-Pastor).

0378-4371/02/$ - see front matter
PII: S0378-4371(02)00809-9

phenomena as adsorption and diffusion of diatomic molecules [4], magnetism [5,6], etc. The occupational degeneracies obtained provide the information to construct the partition function that permits the calculation of the thermodynamic quantities of interest.

The difficulty in treating such systems is that there is statistical correlations in the sense that if a site is occupied, then, at least one of its nearest-neighbor sites must also be occupied. Consequently, there is a distribution of pair of occupied sites. Exact solutions have been found for the one-dimensional case [7–9]. For higher dimensionality, exact solutions have been obtained for special cases, using Pfaffians [10,11] and the matrix transfer method [12,13]. In other words, from a analytical point of view, either the space have been restricted or approximated methods have been utilized to solve this problem.

On the other hand, computer simulations through Monte Carlo (MC) [14–16] offer a powerful way to analyze and interpretate dimer adsorption data. MC simulation has been used mostly by employing the lattice gas model for the adsorbed monolayers. Among these studies, the structural ordering of interacting dimers has been recently analyzed by Romá et al. [14]. The authors concluded that there are a finite number of ordered structures for dimers with repulsive nearest-neighbor interactions. These ordered structures had been predicted in Ref. [15], where the phase diagram for interacting (attractive and repulsive) dimers on a square lattice was reported. The thermodynamic implications of such structural ordering was demonstrated through the analysis of the adsorption isotherm and the collective diffusion coefficient of dimers with nearest neighbor repulsion [16].

In all previously mentioned cases, the surface is considered to be chemically homogeneous and smooth. However, in contrast to the statistic for the simple particles, the degeneracy of arrangements of dimers is strongly influenced by the structure of the lattice space. Although the structure of lattice space plays such a fundamental role in determining the statistics of dimers, there exist very few theories on dimer adsorption on heterogeneous adsorbents [17–22] with: (i) different number of nearest-neighbor sites (different geometries), or (ii) different topographies. Among these theories, one of the most widely used is the Nitta model [17,18], which permits only to study adsorption of polyatomic molecules on random heterogeneous surfaces (RHS). It is clear that the RHS is a limit case (occurring only rarely in real systems), and more general topographies must be considered. For these reasons, it is of interest and of value to inquire how a specific lattice structure (heterogeneous surfaces with intermediate correlations or with different geometries) influences the main thermodynamic properties of adsorbed dimers.

From the experimental point of view, most adsorbates consist of a number of single k components or elementary units, the so-called k-mers. Even the simple gases such as oxygen, nitrogen and carbon monoxide are polyatomic. Furthermore, surfaces generally present inhomogeneities due to irregular arrangement of surface and bulk atoms or the presence of various chemical species, which can significantly affect the entropic contribution to the adsorbate's free energy. Typical examples are O_2, N_2, CO, CO_2, ethane, isobutane, ethylene absorbed in carbon and zeolite molecular sieves [20,23–27], oligomers in activated carbons [20,28], etc. As a first step, the understanding of simple

models, including heterogeneity and multisite occupancy, might be a help and a guide to establish a general framework for the study of this kind of systems.

In this context, this paper has two main objectives: (1) to determine, via MC simulation in grand canonical ensemble and the Fermi–Dirac (F–D) theoretical model presented in a previous article [29], the general properties of the adsorption of dimers on bivariate surfaces with a characteristic correlation length, l, and find out to what extent this length scale could be determined from adsorption measurements. Our bivariate surfaces are composed by two kinds of sites, say shallow and deep sites with adsorptive energies ε_S and ε_D, respectively, arranged in patches of size l. A special class of bivariate surfaces, with a chessboard structure, has been observed recently to occur in a natural system [30], although it was already intensively used in modeling adsorption and surface diffusion phenomena [31,32]. (2) To study the effect of the surface geometry on the properties of adsorption presented in (1). For this purpose, homonuclear dimers adsorbed on square, triangular and honeycomb heterogeneous bivariate lattices are studied.

The plan of the rest of paper is as follow. In Section 2 the lattice-gas model is given along with the basis of the MC simulation of dimer adsorption in the grand canonical ensemble (MCGCE). The theoretical model (F–D approach) is derived in Section 3. The behavior of the simulated adsorption isotherms in comparison with the F–D model, is discussed in Section 4. Section 5 is dedicated to the determination of general scaling properties leading to power-law behavior and to the discussion of its implicances in the determination of l from experimental measurements. We close this article in Section 6 with the conclusions.

2. Basic definitions: the lattice-gas model and MC simulation

We consider the adsorption of homonuclear dimers on square, triangular and honeycomb heterogeneous bivariate lattices. The dimer molecule is composed of two identical segments in a linear array with constant bond length equal to the lattice constant a. The dimers can only adsorb flat on the surface occupying two lattice sites (each lattice site can only be single occupied).

The substrate has been represented by a square, triangular or honeycomb lattice of $M = L \times L$ adsorptive sites, with periodical boundary conditions. The heterogeneity was introduced by considering two kinds of adsorptive sites, deep and shallow traps, in equal concentration ($f_D = f_S = 0.5$) and according to a bimodal site-energy distribution (see Fig. 1). The interaction energies between one dimer's segment and a deep or shallow site are denoted by ε_D or ε_S, respectively. The solid heterogeneous surface is modeled as a collection of finite homotatic patches where each patch is assumed to be a domain of equal size $M_P = l \times l$. These adsorptive domains were used to generate substrates, having different geometrical structure: (i) random distribution of patches, and (ii) chessboard-like array. These energetic topographies had been qualitatively represented in Fig. 2(a), (b) and (c), for squares, honeycomb and triangular lattices, respectively. The black (white) symbols correspond to deep (shallow) adsorption sites; parts (a) and (b) represent random and patchwise case, respectively.

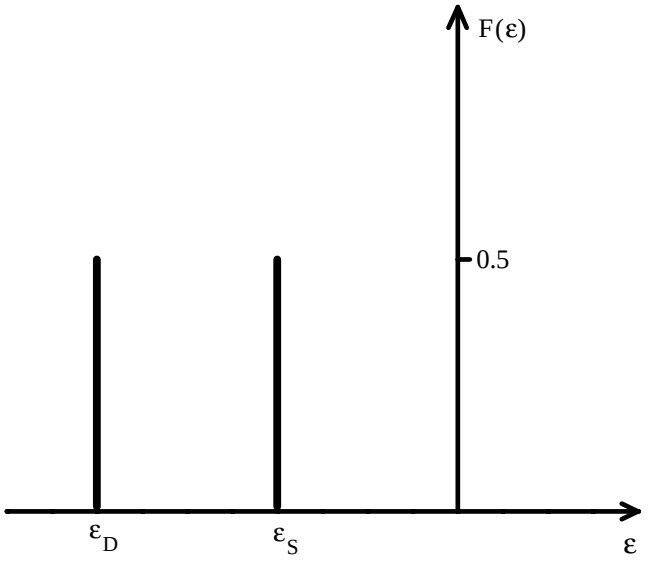

Fig. 1. Bimodal distribution of the adsorptive energies, ε_D and ε_S.

In order to describe a system of N dimers adsorbed on M sites at a given temperature T, let us introduce the occupation variable c_i which can take the values $c_i = 0$ or 1, if the site i is empty or occupied by a dimer unit, respectively. The dimers retain its structure upon adsorption, desorption and diffusion. The Hamiltonian of the system is given by

$$H = \sum_i (\varepsilon_i - \mu) c_i \,, \tag{1}$$

where ε_i ($=\varepsilon_D$ or ε_S) is the adsorption energy of a segment on a i site and μ is the chemical potential.

The adsorption process is simulated through a MCGCE method [29,33]. The mean coverage θ is obtained as simple averages

$$\theta = \frac{1}{M} \sum_i^M \langle c_i \rangle = \frac{2\langle N \rangle}{M} \,, \tag{2}$$

where $\langle N \rangle$ is the mean number of adsorbed particles, and $\langle \ldots \rangle$ means the time average over the MC simulation runs.

3. Adsorption results

The computational simulations have been developed for square, honeycomb and triangular $L \times L$ lattices, with $L = 144$ and periodic boundary conditions. With this lattice size we verified that finite-size effects are negligible. The equilibrium state can be

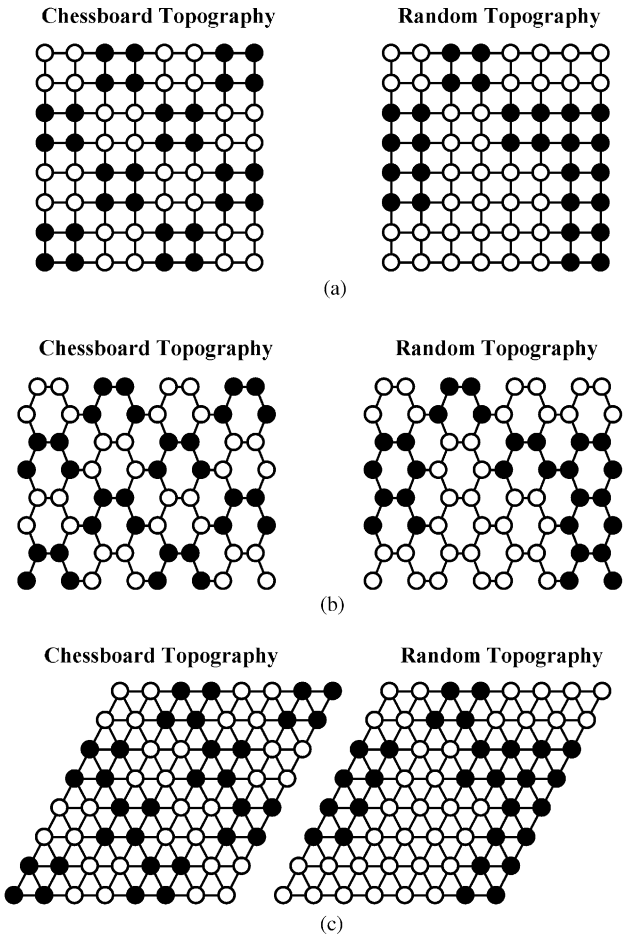

Fig. 2. Schematic representation of heterogeneous bivariate surfaces with chessboard and random topographies: (a) square lattice; (b) honeycomb lattice; and (c) triangular lattice. The patch size in this figure is $l = 2$. The black (white) symbols correspond to deep (shallow) adsorption sites.

well reproduced after discarding the first 10^5–10^6 Monte Carlo step (MCS) [an MCS is achieved when M pair of sites have been tested to change its occupancy state]. Then, averages are taken over 10^5–10^6 successive configurations. It should be noted that displacement (diffusional relaxation) of ad-particles to nearest-neighbor positions, by either jumps along the dimer axis or repetition by rotation around the dimer end, must be allowed in order to reach equilibrium in a reasonable time.

Adsorption of non-interacting dimers on bivariate heterogeneous surface presents a rich and complex behavior depending on the linear size of the patches l, the topological distribution of the patches and the difference between the energies of the patches, $\Delta\varepsilon = \varepsilon_D - \varepsilon_S$.

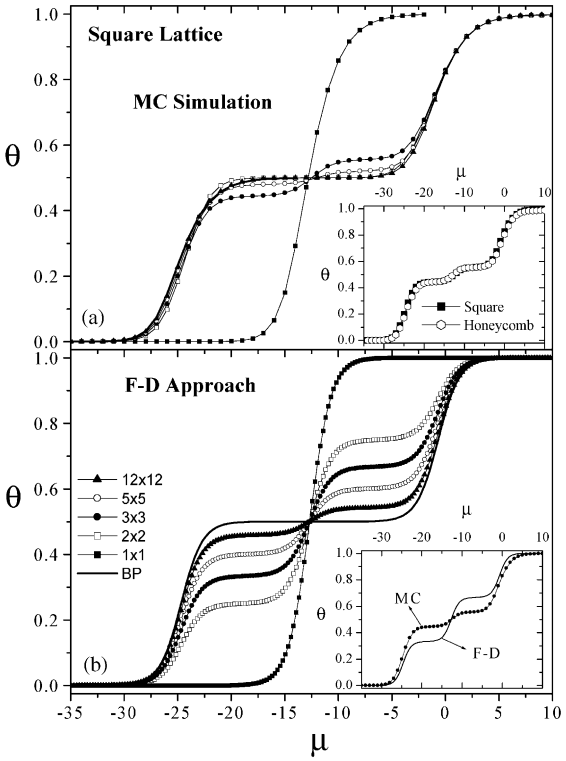

Fig. 3. Adsorption isotherms for square chessboard topographies with different l's and $\Delta E = 12$. (a) [(b)] shows the Monte Carlo (theoretical) results. The inset in (a) [(b)] presents the comparison between isotherms for honeycomb and square lattices with chessboard topography [the two employed methodologies] in a particular case ($l = 3$).

In Fig. 3(a), we show a set of non-interacting dimer isotherms for chessboard bivariate square surfaces with $f_D = f_S = 0.5$, $\Delta\varepsilon/k_BT = 12$ and different sizes of the patches ($l = 1, 2, 3, 5, 12$). In addition, we have plotted the adsorption isotherm corresponding to two big patches (called *BP* in the figure) and the same value of $\Delta\varepsilon$.

Depending on l and the topography, the isotherms present one, two or three different coverage regimes associated to the three possible adsorption energies of a dimer: (i) ε_{DD}, (ii) ε_{SS}, corresponding to a dimer adsorbed on two deep [shallow] sites, and (iii) ε_{SD}, corresponding to a dimer adsorbed on a pair of deep-shallow nearest-neighbor sites. The crossovers between the regimes appear as plateaus at different coverages.

From Fig. 3(a), it is possible to distinguish three different types of isotherms:

(1) For $l = 1$, the dimers are always adsorbed on *DS* pairs and a unique regime characterizes the whole adsorption process.

(2) For even l and two big patches, two marked regimes of adsorption appear: for $0 < \theta < 0.5$, the ad-molecules adsorb on *DD* pairs occupying completely the deep

patches; for $0.5 < \theta < 1$, the shallow sites (*SS* pairs) are occupied until the full coverage is reached. A plateau at $\theta = 0.5$ separates the two regimes:

(3) For odd l (and $l \neq 1$), the number of sites in the deep (and shallow) patches is also odd. For this reason, each patch can be not fulfiled for dimers and empty *DS* pairs, occurring in the borderline between the patches, are involved in the adsorption process. Then, the filling process is as follows: at low values of chemical potential, the *DD* pairs are preferentially occupied by the dimers (regime 1); as the chemical potential increases, *DS* pairs start to be occupied (regime 2); finally, for high values of chemical potential, the *SS* pairs are filled (regime 3). Therefore, the isotherms present three adsorption regimes and two plateaus. Other situation occurs if l is increased. In this case, only two regimes prevail. This is so, due that the number of *DS* pairs, eventually appearing in the borders between the patches, is negligible compared with *SS* or *DD* pairs and do not a big influence on the process.

The isotherms for honeycomb lattices are identical to those obtained from square lattices due to the distribution of pairs *DD*, *DS* and *SS* is the same for honeycomb or square lattices (see the appendix). This situation is shown in the inset of Fig. 3(a) for a particular case ($\Delta\varepsilon = 12$; $l = 3$).

To complete the analysis of Fig. 3(a), it is interesting to note that all curves are contained between two limit ones: the one corresponding to 1×1 patches and the one corresponding to two big patches.

For dimers adsorbed on chessboard bivariate surfaces with triangular geometry [Fig. 4(a)], the filling mechanism can be explained based on the same argument used above [Fig. 3(a)]. In this case, the high connectivity of the lattice allows to cover completely the pairs *DD* (for all values of l) and the resulting isotherms present only two regimes of adsorption as in the *BP* case.

The isotherms corresponding to random bivariate heterogeneous surfaces have been not shown in Figs. 3 and 4 for reasons of simplicity. The unique difference between random and patchwise topographies is the following: for fixed l, the chessboard-like topography presents a larger value of the interface between deep and shallow patches compared with the corresponding random topography. Consequently, the number of *DS* pairs (and the width in coverage of the regime 2) is, for the ordered topography, bigger than for the random surface.

4. F–D approach for the dimer adsorption isotherm on bivariate surfaces

Let us consider an adsorbate molecule of two identical monomers. Let us further assume adsorption sites with two possible different energies ($\varepsilon_D, \varepsilon_S$). The total adsorption energy for a particular dimer, ε_2, is

$$\varepsilon_2 = \sum_{i=1}^{2} \varepsilon_i \,, \tag{3}$$

where each monomer occupies a single adsorption site.

Considering that each of the two terms of the above sum can have any of two values $\varepsilon_D, \varepsilon_S$, the number of "energy levels" for ε_2 (regardless of its degeneracy) is

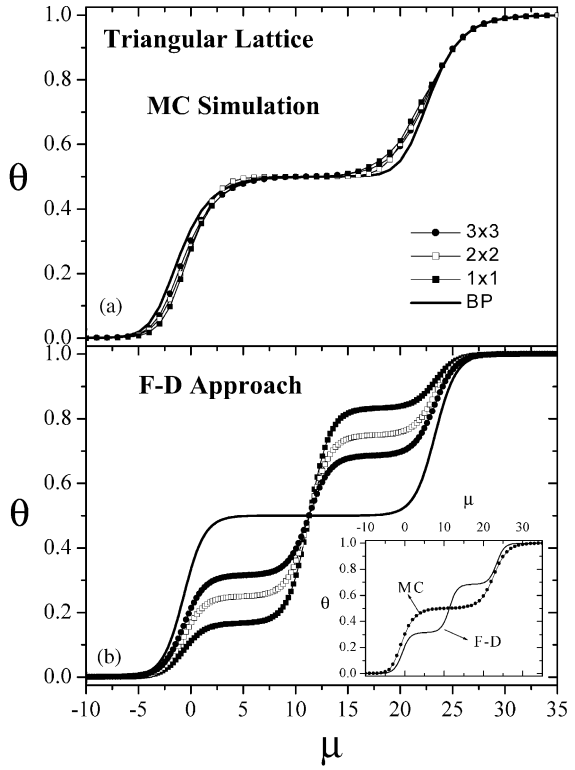

Fig. 4. As Fig. 3 for triangular lattices and the l's indicated in the figure.

four. Under the hypothesis that these energy levels are different from each other, their occupation number is $S_i = 0$ or 1 for $i = 1,\ldots,4$.

The mean occupation number of a level $\varepsilon_2, \theta(\varepsilon_2)$, is then given by the F–D statistics [34]

$$\theta(\varepsilon_2) = \frac{\exp(-(\varepsilon_2 - \mu)/kT)}{1 + \exp(-(\varepsilon_2 - \mu)/kT)}\,. \tag{4}$$

Eq. (4) represents the local adsorption isotherm on a set of two sites. The mean surface coverage $\bar{\theta}$ is then obtained by averaging out over $f(\varepsilon_2)$

$$\bar{\theta} = \sum_{i=1}^{4} f(\varepsilon_2^i)\theta(\varepsilon_2^i) \tag{5}$$

with ε_2^i being the energy of the ith level.

The function $f(\varepsilon_2^i)$ can be symbolically expressed in terms of the frequencies f_D and f_S

$$f(\varepsilon_2^i) = f(f_D, f_S)\,. \tag{6}$$

Analytical expressions for $f(\varepsilon_2^i)$ can be written down by supposing a particular adsorption sites topography. For dimers on a surface with two kinds of adsorption sites, $f(\varepsilon_2^i)$ can take four possible values:

$$\begin{aligned} f(\varepsilon_2^1) = f_{DD} \quad & (\text{fraction of pairs of } (i,j) \text{ nearest neighbor sites} \\ & \text{with } \varepsilon_i = \varepsilon_j = \varepsilon_D)\,, \\ f(\varepsilon_2^2) = f_{DS} \quad & (\text{fraction of pairs of } (i,j) \text{ nearest neighbor sites} \\ & \text{with } \varepsilon_i = \varepsilon_D \text{ and } \varepsilon_j = \varepsilon_S)\,, \\ f(\varepsilon_2^3) = f_{SD} \quad & (\text{fraction of pairs of } (i,j) \text{ nearest neighbor sites} \\ & \text{with } \varepsilon_i = \varepsilon_S \text{ and } \varepsilon_j = \varepsilon_D)\,, \\ f(\varepsilon_2^4) = f_{SS} \quad & (\text{fraction of pairs of } (i,j) \text{ nearest neighbor sites} \\ & \text{with } \varepsilon_i = \varepsilon_S = \varepsilon_S)\,, \end{aligned} \tag{7}$$

being $f_{DS} = f_{SD}$.

Then, a simple isotherm equation is obtained for the general case of correlated topography:

$$\begin{aligned} \bar{\theta}(\mu,T) = f_{DD}\frac{\exp\left[-\frac{(2\varepsilon_D-\mu)}{kT}\right]}{1+\exp\left[-\frac{(2\varepsilon_D-\mu}{kT}\right]} + 2f_{DS}\frac{\exp\left[-\frac{(\varepsilon_D+\varepsilon_S-\mu}{kT}\right]}{1+\exp\left[-\frac{(\varepsilon_D+\varepsilon_S-\mu}{kT}\right]} \\ + f_{SS}\frac{\exp\left[-\frac{(2\varepsilon_S-\mu)}{kT}\right]}{1+\exp\left[-\frac{(2\varepsilon_S-\mu}{kT}\right]}\,. \end{aligned} \tag{8}$$

The effect of intermediate topographies can be easily investigated in the framework of the F–D approach. In the particular case of chessboard and random patches topographies, f_{DD}, f_{DS} and f_{SS} can be obtained from geometrical arguments (see the appendix),

$$\begin{aligned} & f_{DD}^{rand} = \frac{l-1}{2l}, \quad f_{DS}^{rand} = \frac{1}{2l}, \quad f_{SS}^{rand} = \frac{l-1}{2l}\,, \\ & f_{DD}^{chess} = \frac{2l-1}{4l}, \quad f_{DS}^{chess} = \frac{1}{4l}, \quad f_{SS}^{chess} = \frac{2l-1}{4l}\,. \end{aligned} \tag{9}$$

In order to compare the present model's predictions with simulation, we used the parameters as in Figs. 3(a) and 4(a). Although there is a strong quantitative difference between the analytical [Figs. 3(b) and 4(b)] and simulated isotherms, the qualitative behavior seems to be the same: in fact, (i) both isotherms present different coverage regimes, separated by well-defined plateaus and (ii) all isotherms are contained between two limit curves (1×1 and BP).

As it can be seen from the insets of Figs. 3(b) and 4(a), for a particular case ($l=3$), the theoretical model reproduces fairly well the two-steeped behavior of the simulated isotherm for the square lattice, while predicts a more steeped isotherm for the triangular case.

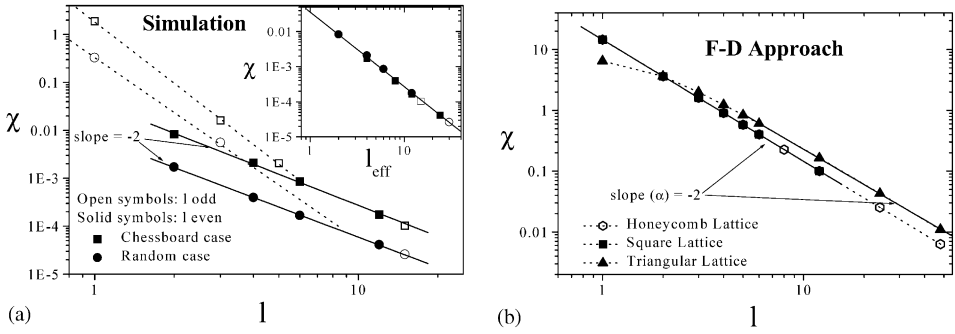

Fig. 5. Power-law behavior of the quantity χ showing the data for chessboard topographies: (a) computational results for square lattices; and (b) theoretical results for square, triangular and honeycomb lattices. The symbology is indicated in the figure. In the inset of (a) we present the collapse of data for different topographies on a single curve when the effective length scale l_{eff} is used.

The differences between analytical and computational results is directly associated to the theoretical hypothesis considering pairs independent on the lattice. In fact, in the real (and simulated) process, the pairs are not independent. For example, the adsorption of a isolated dimer on a determined pair of *NN* sites, eliminates six possible adsorption pairs for the next incoming dimer.

Finally, it is important to note that even though Eq. (8) was derived for the case of molecules made of identical atoms or chemical groups, this can be generalized to take in account larger molecules with two or more kinds of atoms.

5. Scaling behavior

The fact that adsorption isotherm curves for different values of the length scale vary between two limit curves (see Figs. 3 and 4) allows to define the following quantity:

$$\chi = \left[\int_{-\infty}^{\infty} |\theta(\mu) - \theta^R(\mu)| \, \mathrm{d}\mu \right]^2 , \tag{10}$$

where $\theta^R(\mu)$ is the reference adsorption isotherm. This quantity, χ, which represents the area between a given curve and a reference curve, is appropriate to measure the deviation among the isotherms and study its behavior as the length scale is varied. By taking as a reference curve the one corresponding to the *BP* topography, we obtain Fig. 5(a). In this figure we can see that χ behaves as a power law in l with exponent $\alpha = -2$. Same deviations appears for small (and even) values of l due to the patches cannot be fulfiled for dimers and the number of *DS* pairs in the borderline between the patches affects considerably the adsorption process. These deviations disappears as l is increased and the effect of the *DS* pairs is negligible. Identical value for α is obtained by using: (i) other reference curve (like for example the theoretical F–D isotherm for *BP* topography); (ii) other connectivity; and (iii) other value of $\Delta\varepsilon$.

It is interesting to note (see Fig. 5) that the exponent α is the same for chessboard and random topography (logarithmic plots are parallel). This suggest the idea that a random topography characterized by a scale length l behaves like a chessboard topography with a larger scale length. Straightforward calculations (see the appendix) demonstrate that chessboard and random topography curves for χ should become the same curve as a function of an effective length scale (representing an effective patch size), l_{eff}, given by

$$l_{eff} = sl\,, \tag{11}$$

where $s=1$ for chessboard topography and $s=2$ for random topography. In the inset of Fig. 5(a) we can see for the case of χ how the simulation data for different topographies cast over a single curve, for a given regime, when the effective length scale is used.

In Fig. 5(b) we study the scaling behavior of adsorption in the framework of F–D approximation. We find that the same scaling law [as given in Fig. 5(a)] is obeyed, with exponent $\alpha=-2$. The behavior of χ for the analytical approach is in excellent agreement with the behavior observed by MC simulations, which reinforce the robustness of the scaling law introduced in this paper.

Finally, it is possible to establish that the quantity χ, calculated for the adsorption isotherm by using either a theoretical or a simulated reference curve, behaves as a power law in the effective length scale

$$\ln\chi = const. + \alpha \ln l_{eff}\,, \tag{12}$$

where the exponent α has an universal behavior given by $\alpha=-2$. This result provide a method for the characterization of the energetic topography of heterogeneous substrates which can be approximated by bivariate surfaces, through adsorption measurements of non-interacting dimers. In fact, by choosing an appropriate theoretical approach as a reference curve, the value of χ can be calculated allowing l_{eff} to be obtained from Eq. (11). A similar study for interacting dimers is in progress.

6. Conclusions

In this work we have studied, by using Monte Carlo simulation and theoretical modeling, the adsorption of homonuclear dimers on two-dimensional bivariate surfaces. The heterogeneous substrate has been modeled as an array of deep and shallow sites, with energies ε_D and ε_S, forming $l \times l$ patches distributed at random or in chessboard-like ordered domains on a square, honeycomb and triangular lattice.

In order to analyze the effects of the topography on the adsorption process, three quantities have been chosen as the control parameters: (i) the size of the patches, l, which is associated to the correlation length; (ii) the topological distribution of the patches (at random or in chessboard structure) and (iii) the connectivity of the lattice, c ($c=3,4,6$). On this basis, different cases have been observed:

(1) For $c=3,4$ and chessboard topography with $l=1$, only one adsorption regime appears corresponding to the filling of *DS* pairs.

(2) For $c = 3, 4$ and chessboard topography with odd l, the isotherms present two regimes, corresponding to the sequential filling of *DD* and *SS* pairs (also this behavior is observed for *BP*).

(3) For $c = 3, 4$ and chessboard topography with even l, three regimes are present in the isotherms, the corresponding to the sequential filling of *DD*, *DS* and *SS* pairs. In addition, when l increases the fraction of *DS* pairs decreases (particularly, for $l \geqslant 3$ the fraction of *DS* pairs is practically negligible and the isotherms are very close to the corresponding to two big patches).

(4) For $c = 6$, two adsorption regimes appears corresponding to the sequential filling of *DD* and *SS* pairs. In all cases, the random topography minimizes the borderline between deep and shallow patches, diminishing the number of *DS* pairs, and for this reason, the width in coverage of the regime 2.

For all cases, unique scaling properties have been established for the adsorption isotherms. The exponent α is found to follow a universal behavior, in the sense that it is independent of the topography (chessboard or random), the $\Delta\varepsilon$ and the connectivity. In addition, we have found that this universality goes far beyond. In fact, exactly the same behavior is found by taking different isotherms as reference curves for the calculation of χ.

These findings provide for the first time a method to characterize the energetic topography (i.e., obtain the parameters from experimental measurements) of a class of heterogeneous surfaces which can be approximately represented as bivariate surfaces.

Acknowledgements

It is a pleasure to acknowledge many helpful and stimulating discussions with F. Bulnes and G. Zgrablich. This work is partially supported by Fundación Antorchas.

Appendix

We introduce the following general notation: let f_{ij} be the number of *NN* pairs of sites of type (i,j) [i or j takes the values D (deep), S (shallow)], n_k^{ij} be the number of *NN* pairs of sites of type (i,j) on patches of type k, n_{ci}^{ii} be the number of *NN* pairs of type (i,i) corresponding to the contact between two patches of type i, n be the total number of *NN* pairs, N_i be the number of patches of type i and N_{ci} be the mean number of contacting patches of type i.

Then, for a square lattice of size L with a chessboard topography of patches of sites D and S, each of size l, the fraction of pairs of *NN* sites of type *DD*, f_{DD}, is given by

$$f_{DD} = \frac{n_D^{DD} N_D}{n} \,. \tag{A.1}$$

Now, in our model

$$n_D^{DD} = 2(2l-2)^2 + 6(2l-2) + 4 \,, \tag{A.2}$$

Table A.1

Square lattice			
$f_{DD}^{chess} = f_{SS}^{chess}$	f_{DS}^{chess}	$f_{DD}^{rand} = f_{SS}^{rand}$	f_{DS}^{rand}
$\frac{l-1}{2l}$	$\frac{1}{2l}$	$\frac{2l-1}{4l}$	$\frac{1}{4l}$
Honeycomb lattice			
$f_{DD}^{chess} = f_{SS}^{chess}$	f_{DS}^{chess}	$f_{DD}^{rand} = f_{SS}^{rand}$	f_{DS}^{rand}
$\frac{l-1}{2l}$	$\frac{1}{2l}$	$\frac{2l-1}{4l}$	$\frac{1}{4l}$
Triangular lattice			
$f_{DD}^{chess} = f_{SS}^{chess}$	f_{DS}^{chess}	$f_{DD}^{rand} = f_{SS}^{rand}$	f_{DS}^{rand}
$\frac{3l^2-4l+2}{6l^2}$	$\frac{8l-4}{6l^2}$	$\frac{6l^2-4l+1}{12l^2}$	$\frac{8l-2}{12l^2}$

$$N_D = \frac{1}{2}\left(\frac{L}{2l}\right)^2 = \frac{L^2}{8l^2}\,, \tag{A.3}$$

$$n = 2L^2 \tag{A.4}$$

so that from Eqs. (A.1)–(A.4) we obtain

$$f_{DD}^{chess} = \frac{l-1}{2l}\,. \tag{A.5}$$

On the other hand, for a random topography of patches of size l, we have

$$f_{DD} = \frac{n_D^{DD} N_D + n_{cD}^{DD} N_{cD}}{n}\,. \tag{A.6}$$

In this case

$$n_D^{DD} = 2(l-2)^2 + 6(l-2) + 4\,, \tag{A.7}$$

$$N_D = \frac{1}{2}\left(\frac{L}{l}\right)^2, \tag{A.8}$$

$$N_{cD} = \frac{1}{2}\left(\frac{L}{l}\right)^2 \tag{A.9}$$

so that, replacing Eqs. (A.4) and (A.7)–(A.9) in Eq. (A.6), we obtain f_{DD} for a random topography

$$f_{DD}^{rand} = \frac{2l-1}{4l}\,. \tag{A.10}$$

By similar arguments it is possible to obtain f_{ij} in all the studied cases. The results are listed in Table A.1.

References

[1] R.H. Fowler, G.S. Rushbrooke, Trans. Faraday Soc. 33 (1937) 1272.
[2] P.J. Flory, J. Chem. Phys. 10 (1942) 51.
[3] P.J. Flory, Principles of Polymers Chemistry, Cornell University Press, Ithaca, New York, 1953.
[4] T.T. Tsong, R. Casanova, Phys. Rev. B 21 (1980) 4564;
T.T. Tsong, R. Casanova, Phys. Rev. B 22 (1980) 4632.
[5] L.N. Cooper, Phys. Rev. 104 (1959) 1189.
[6] J.M. Koterlitz, D.J. Thouless, J. Phys. C 5 (1972) L124.
[7] D. Lichtman, R.B. McQuistan, J. Math. Phys. 8 (1967) 2441.
[8] R.B. McQuistan, Il Nuovo Cimento B 58 (1968) 86.
[9] A.J. Ramirez-Pastor, T.P. Eggarter, V. Pereyra, J.L. Riccardo, Phys. Rev. B 59 (1999) 11027.
[10] H.N.V. Temperley, M.E. Fisher, Phil. Mag. 6 (1961) 1061.
[11] P.W. Kasteleyn, Physica 27 (1961) 1209.
[12] E.H. Lieb, J. Math. Phys. 8 (1967) 2339.
[13] A.J. Phares, F.J. Wunderlich, D.W. Grumbine, J.D. Curley, Phys. Lett. A 173 (1993) 365.
[14] F. Romá, A.J. Ramirez-Pastor, J.L. Riccardo, J. Chem. Phys. 24 (2001) 10932.
[15] A.J. Ramirez-Pastor, J.L. Riccardo, V. Pereyra, Surf. Sci. 411 (1998) 294.
[16] A.J. Ramirez-Pastor, M.S. Nazzarro, J.L. Riccardo, V. Pereyra, Surf. Sci. 391 (1997) 267.
[17] T. Nitta, H. Kiriyama, T. Shigeta, Langmuir 13 (1997) 903.
[18] T. Nitta, M. Kuro-oka, T. Katayama, J. Chem. Eng. Jpn. 17 (1984) 45;
T. Nitta, A.J. Yamaguchi, J. Chem. Eng. Jpn. 25 (1992) 420.
[19] A.W. Marczewski, M. Derylo-Marczewska, M.J. Jaroniec, J. Colloid Interface Sci. 109 (1986) 310.
[20] W. Rudziński, D.H. Everett, Adsorption of Gases on Heterogeneous Surfaces, Academic Press, New York, 1992.
[21] W. Rudziński, K. Nieszporek, J.M. Cases, L.I. Michot, F. Villeras, Langmuir 12 (1996) 170.
[22] M. Borówko, W. Rżysko, J. Colloid Interface Sci. 182 (1996) 268;
M. Borówko, W. Rżysko, Ber. Bunsenges. Phys. Chem. 101 (1997) 84.
[23] O. Talu, I. Zwiebel, A.I.Ch.E. J. 32 (1986) 1263.
[24] S.H. Hyun, R.P. Danner, J. Chem. Eng. Data 27 (1982) 196.
[25] G.W. Miller, K.S. Knaebel, K.G. Ikels, A.I.Ch.E. J. 34 (1987) 2.
[26] D. Razmus, C. Hall, A.I.Ch.E. J. 37 (1991) 5.
[27] A.M. Goulay, J. Tsakiris, E. Cohen de Lara, Langmuir 12 (1996) 371.
[28] R.A. Koble, T.E. Corrigan, Ind. Eng. Chem. 44 (1952) 383.
[29] A.J. Ramirez-Pastor, M.S. Nazzarro, J.L. Riccardo, G. Zgrablich, Surf. Sci. 341 (1995) 249.
[30] T.W. Fishlock, J.B. Pethica, R.G. Egdell, Surf. Sci. L 47 (2000) 445.
[31] F. Nieto, A.J. Ramirez-Cuesta, R. Faccio, Phys. Rev. E 59 (1999) 3706.
[32] F. Nieto, C. Uebing, V. Pereyra, R. Faccio, Surf. Sci. 423 (1999) 256.
[33] N. Metropolis, A.W. Rosenbluth, M.N. Rosenbluth, A.W. Teller, E. Teller, J. Chem. Phys. 21 (1953) 1087.
[34] D.A. Mc. Quarrie, Statistical Mechanics, Harper Collins Publishers, New York, 1976.